Spectral analysis of Brazilian data and comparison with ground-motion models

Stéphane Drouet (Observatório Nacional Rio de Janeiro, Brasil), and Marcelo Assumpção (IAG/USP, São Paulo, Brasil)

This paper was prepared for presentation during the 13th International Congress of the Brazilian Geophysical Society held in Rio de Janeiro, Brazil, August 26-29, 2013.

Abstract

In this study, data from 13 earthquakes that occurred in South-East and North-East Brazil are analysed, with magnitude ranging from 2.6 to 5.2 and hypocentral distance from 1.5 to 891 km. Fourier spectra are computed in order to determine source, attenuation and site parameters. First, the high frequency decay of the Fourier spectra is investigated. It reveals that anelastic attenuation is very weak in Brazil leading to very little high-frequency attenuation as compared to more active regions. Second, the attenuation of Fourier spectra at around 1 Hz shows that geometrical decay is close to one. After correction for attenuation the source Fourier spectra are use in a non-linear inversion scheme in order to determine moment magnitude and corner frequencies, and subsequently estimate stress drop for these events. Inverted moment magnitude are much smaller than body-wave magnitudes included in the earthquake catalog, and stress drops range between about 0.1 and 1 MPa. This new information help to compare recorded response spectra and those predicted by Ground-Motion Prediction Equations.

Introduction

One of the key ingredients in seismic hazard analysis is the ground-motion prediction equation (GMPE) which relates recorded ground-motion amplitude to some source parameters (magnitude, style-of-faulting...), propagation path parameters (source-to-site distance), and site parameters (classification, superficial S-wave velocity...).

Such equations are usually determined empirically from regression analyses, which require large data bases of records covering a broad magnitude and distance range. Consequently, in regions of low-to-moderate seismicity no such GMPEs are available due to the lack of data.

One question is then to judge the ability of GMPEs developed in one region to predict ground-motion in another region. Comparison of recorded data, even if only a few of them is available, with GMPEs may help to do so (Scherbaum et al., 2004, 2009). These methods rely on statistical analysis of the residuals between observed and predicted response spectra.

In order to perform such a comparison, the metadata that describes the source, the propagation and the site need also to be accurately known. Indeed, GMPEs are not homogeneous in terms of predictor variables. For examples, there exists different scales of magnitude and different source-to-site distances measures (Cotton et al., 2006). Moreover, site characteristics may be taken into account through site classes or other measures like the near surface S-wave velocity which is generally averaged over 30 meters (v_{S30}).

These metadata can be inferred from Fourier spectral analysis of recorded data. In particular moment magnitudes (M_w) which is becoming the most widely used magnitude scale can be determined (Drouet et al., 2010).

In this study the data are analysed following a sequence of steps. First, the high-frequency decay of the Fourier spectra (Hanks, 1982; Anderson and Hough, 1984) is investigated in order to estimate a regional quality factor (anelastic attenuation), and determine the station-dependent high-frequency decay (κ_0). For rock sites there is a correlation with the stiffness of the layers underlying the station (Van Houtte et al., 2011). Consequently, this parameter helps us to assess to site characteristics of the recording stations. Second, the attenuation of the Fourier spectra at 1 Hz helps us to estimate the rate of geometrical decay. Third, the records of each events are corrected from attenuation and source spectra are estimated from which both seismic moment (which is converted to M_w using Hanks and Kanamori, 1979 relationship) and corner frequency are estimated. Finally, using the estimated M_w and site conditions, response spectra computed from the data are compared to empirical GMPEs.

Data

In this study we use 13 earthquakes recorded in South-East and North-East Brazil with clear P- and S-wave arrival. For these events the earthquake catalog of the IAG reports location and m_b magnitude (Table 1) which range between 2.6 and 5.2. Epicentral distances range from 1.5 to 891 km.

Table 1: Origin date and time, location and mb for the events analysed

N	Date	Time	Lon	Lat	m_B
1	1993/12/04	01:11:05.704	-44.75	-20.26	2.6
2	1993/12/27	22:48:10.800	-44.47	-20.32	3.6
3	1993/12/28	20:47:02.000	-44.47	-20.32	4.0
4	1996/10/18	21:44:01.000	-46.76	-21.05	4.0
5	1997/11/17	17:27:59.990	-45.76	-20.75	3.7
6	2000/09/28	16:04:07.000	-49.05	-20.93	3.4
7	2000/11/20	09:36:25.689	-47.66	-16.07	3.9
8	2006/05/20	04:26:05.670	-36.16	-8.26	3.9

9	2008/04/23	00:00:48.020	-45.44	-25.71	5.2
10	2010/01/11	15:53:55.200	-35.65	-5.55	4.0
11	2010/10/08	20:16:54.060	-49.15	-13.77	5.0
12	2012/12/19	04:50:00.000	-43.88	-16.70	3.6
13	2012/12/19	05:31:17.120	-43.88	-16.70	3.6

Figure 1 shows the events, recording stations and path corresponding to the records analysed in this study.

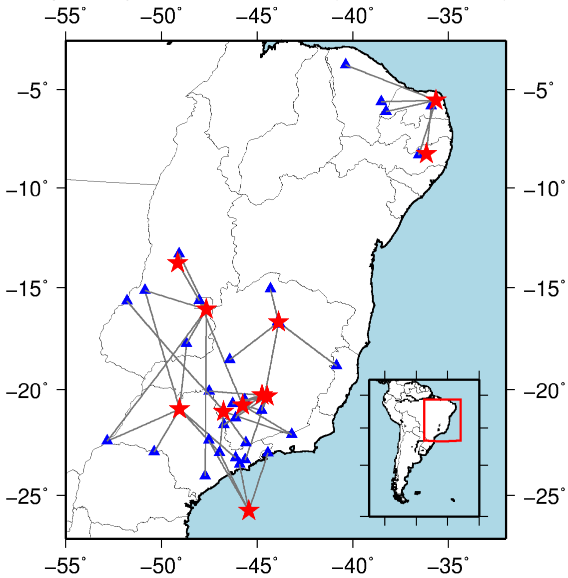

Figure 1: Map of the events (red stars), stations (blue triangles) and propagation paths (grey lines).

For each record, a S-wave window starting from the S-wave arrival and ending at the time for which 95% of the energy is encapsulated in the window. In order to avoid problems linked with very long recordings, the window length is limited to 20 s for distances lower than 50 km, 50 s for distances lower than 500 km, and 100 s for distances greater than 500 km.

A noise window is defined from either the 25 sec before the P-wave arrival minus 5 s, or a window of at least 10 seconds between the beginning of the record and the P wave arrival minus 5 s, or the last 10 seconds of the record, depending on the data available.

Fourier spectra are computed for both the noise and the S-wave window and data are kept if the signal-to-noise ratio is greater than 5. The minimum and maximum usable frequencies are manually picked, but the choice is limited by the signal-to-noise ratio and the Nyquist frequency which varies from record to record from 5 to 50 Hz.

Response spectra are also computed for all the records from the window beginning 10 s before the P-wave arrival and ending 100 s after the S-wave arrival.

Method

Anderson and Hough (1984) proposed a model for the observed high-frequency decay of Fourier spectra:

$$A(f) = \exp(-\pi\kappa f) \text{ for } f \geq f_E$$

where f_E is determined visually and is the frequency above which the Fourier spectra decays linearly in a log(amplitude)-frequency plot. These authors also showed that these kappa values depend on distance since they are related to anelastic attenuation. Analysing various records at different distances allows the estimation of the quality factor at high frequency Q:

$$\kappa(R) = \kappa_0 + \frac{\pi R}{Q v_S}$$

Assuming a Brune's source (Brune 1970, 1971), the far field S-wave acceleration Fourier spectra from earthquake i, recorded at station j and for frequency f_k, can be written as:

$$A_{ijk} = \frac{2R_{\theta\varphi}}{4\pi\rho v_S^3} \frac{M_{0_i} \times (2\pi f_k)^2}{1 + \left(\frac{f_k}{f_{c_i}}\right)^2} \frac{1}{R_{ij}^{\gamma}} \exp\left(\frac{-\pi R_{ij} f_k}{Q_0 f^{\alpha} v_S}\right) S_{jk}$$

where $R_{\theta\Phi}$ is the average S-wave radiation pattern (0.55), ρ is the density at the source (2800 kg/m^3), v_S is the S-wave velocity at the source (3500 m/s), M_{0i} and f_{ci} are the seismic moment and corner frequency for event i, R_{ij} is the hypocentral distance, γ is the geometrical spreading exponent, $Q(f)=Q_0 f^{\alpha}$ is the quality factor, and S_{jk} is the site effect at station j for frequency f_k.

Knowing γ, $Q(f)=Q_0 f^{\alpha}$ and S_{jk}, each spectra can be corrected for attenuation and site effect in order to estimate a source spectra which only depends on seismic moment and corner frequency. Using a non-linear inversion scheme these two source parameters are determined. Moreover, they are used to estimate stress drops for the events following Brune (1970):

$$\Delta\sigma = \frac{7}{16} M_0 \left(\frac{fc^3}{0.37 v_S}\right)$$

Results

Figure 2 shows an example of S-wave and noise Fourier spectra in a log(amplitude)-lin(frequency) plot. It shows that below about 5 Hz the spectra is characterized by a rapid increase of amplitude with frequency until it reaches a maximum and then starts to linearly decrease with increasing frequency, up to about 25 Hz in the example. Above 20-25 Hz the S-wave spectra starts to flatten and we neglected this data even though the signal-over-noise ratio is still good. The minimum and maximum frequencies are picked manually, and kappa is simply evaluated from the slope of the regression of the logarithm of the amplitude versus frequency between these two frequencies. The regression line is shown on Figure 2.

All the records in our data base are investigated in this way and Figure 3 shows the estimated kappa's versus hypocentral distance. The determined kappa's are very low which is characteristic of very hard rock sites typical of Stable Continental Regions (Van Houtte et al., 2011). The negative values shown in the figure are linked with either bad picking of the frequency band, or with spectra that are almost flat due to the very low attenuation. They are however not considered further. The regression of the kappa values against distance allows us to determine the quality factor at high frequency around 10-20 Hz which is found to be close to 4000. Such very high Q indicate a very low anelastic attenuation in the region.

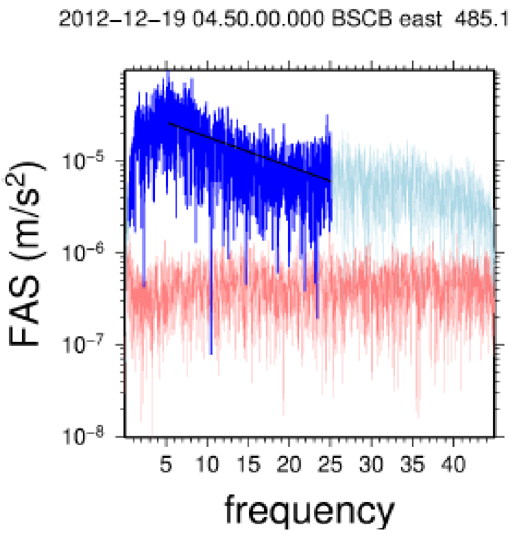

Figure 2: Example of S-wave (blue curve) and noise (red curve) Fourier spectra. The part used to estimated kappa is also shwon (black curve).

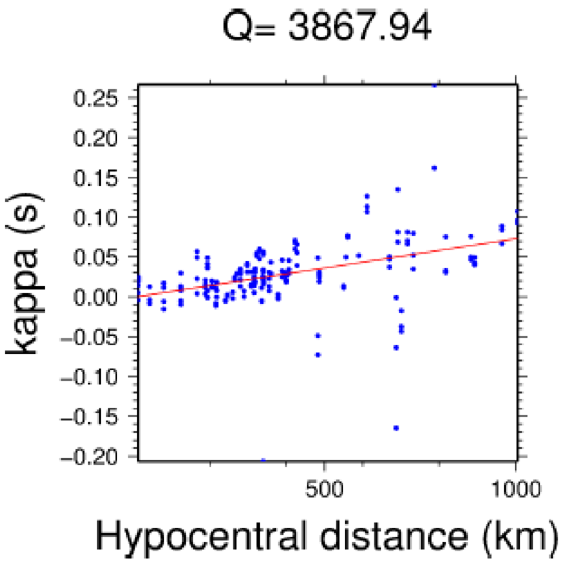

Figure 3: Estimated kappa's for all the records included in the analysis versus hypocentral distance (blue dots). The regression line is shown (red line), the slope of which is used to estimate Q as indicated on top of the picture.

Figure 4 shows the Fourier spectral amplitudes at 1 Hz for all the records. Here, we make the assumption that for all the events the corner frequency is larger than 1 Hz, such that the same part of the spectra is analysed for all the events. For the largest events this assumption may not hold but this should not impact much the results since it is only one event. There is a considerable scatter in the recorded Fourier spectral amplitudes at 1 Hz although since all sites appear to be good rock sites, the site effects should be almost negligible. A more careful inspection of all the spectra and maybe some smoothing may help to reduce this scatter. The regression against distance gives a geometrical exponent close to 0.9. No segmentation linked with Moho reflection can be observed due to the large scatter.

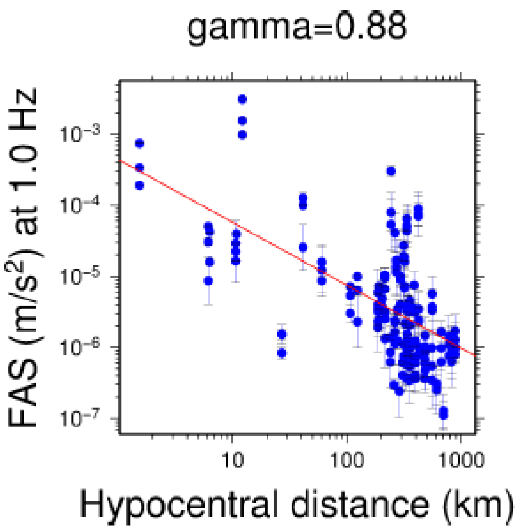

Figure 4: Fourier spectral amplitude at 1 Hz against hypocentral distance (blue dots). The regression from which the geometrical exponent decay is estimated is also shown (red line).

Using the estimated quality factor and geometrical spreading exponent, recorded Fourier spectra are corrected for attenuation. We assume that site effects are negligible. Figure 5 shows an example of corrected Fourier spectra for one of the events.

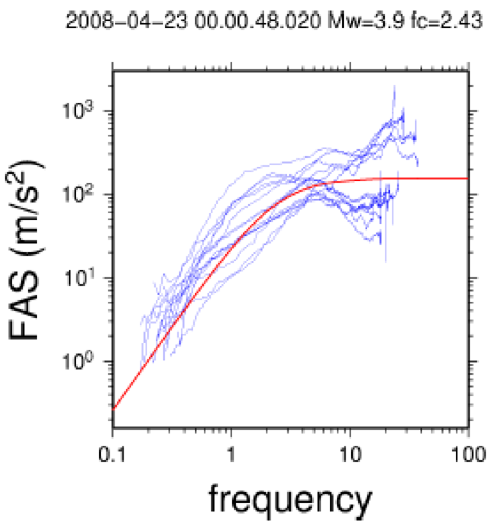

Figure 5: Example of acceleration Fourier spectra corrected for attenuation for each recordings of one of the earthquakes (blue curves). The non-linear fit of the source term is also shown (red line).

Seismic moments and corner frequency are computed from a non-linear fit of the source term using the attenuation corrected spectra. Figure 6 compares the Mw and mb for the 13 earthquakes analysed. Estimated Mw's are smaller by almost one order of magnitude than mb's. Since Mw's are very sensitive to the geometrical spreading exponent some more tests are needed.

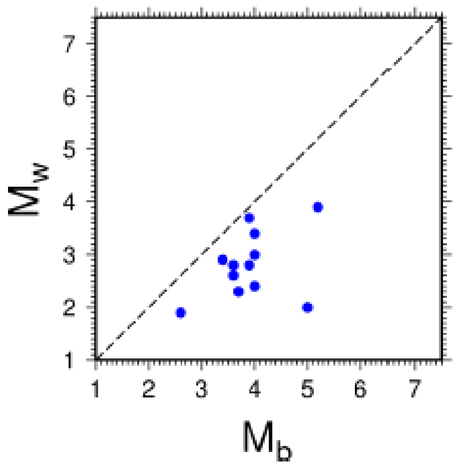

Figure 6: Comparison of moment magnitude and body-wave magitude for the analysed events.

Figure 7 shows the corner frequencies and moment magnitude for the earthquakes used in the present study. Lines of constant stress drop are also shown and stress drops range between 0.1 and 1 MPa.

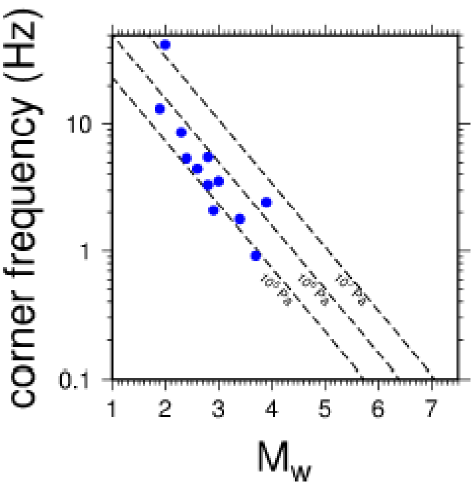

Figure 7: Corner frequencies versus moment magnitudes. Lines of constant stress drop (0.1, 1, and 10 MPa) are also shown.

Finally, we compare the recorded response spectra with a GMPE for stable continental regions: Toro et al. (1997). Figure 8 compares recorded and predicted response spectral amplitude for PGA and for 1.0 s. One difficulty is that the GMPE is evaluated outside its validity range since it was developed for magnitude greater than 5. Such extrapolation may under certain conditions lead to erroneous results which we believe is not the case here since the GMPE is constrained by physical models (it is not purely ampirical).

Figure 8 shows that the GMPE over-predicts PGA for magnitudes below 4. The magnitude scaling is too weak in the model. On the other hand, the distance scaling seems consistent with the data. At 1.0 s, the model seems to perform fairly well.

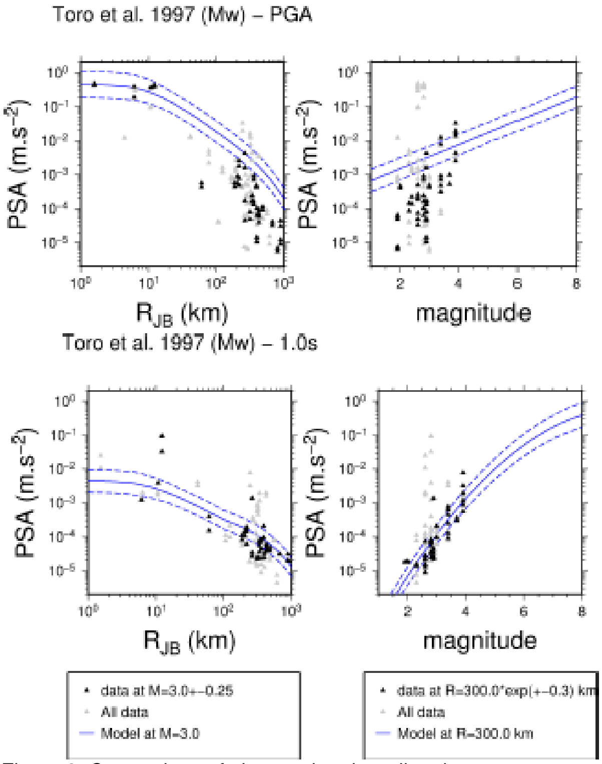

Figure 8: Comparison of observed and predicted response spectral amplitude for PGA (top), and 1.0 s (bottom), against distance (left) and magnitude (right).

Conclusions

This very preliminary analysis of the Brazilian data for seismic hazard analysis shows that valuable information can be extracted from the local recordings even though records from only small magnitudes are available at relatively large distances.

Many parts of the analysis may be improved, including a greater number of data. The long term aim would be to use this data in order to perform stochastic simulations of ground-motion.

Acknowledgments

The authors would like to warmly thank all the members of the teams in the two institutions who contribute to the life of the seismic networks.

References

Anderson, J. G., and S. E. Hough (1984). A model for the shape of the fourier amplitude spectrum of acceleration at high frequencies, Bull. Seismol. Soc. Am. 74, 1969–1993.

Brune, J.N., 1970. Tectonic stress and the spectra of seismic shear waves from earthquakes, J. geophys. Res., 75(26), 4997–5009.

Brune, J.N., 1971. Correction, J. geophys. Res., 76(20), 5002.

Cotton, F., F. Scherbaum, J. J. Bommer, and H. Bungum (2006). Criteria for selecting and adjusting ground-motion models for specific target regions: Application to central Europe and rock sites, Journal of Seismology 10, doi 10.1007/s10950-005-9006-7.

Drouet, S., F. Cotton, and P. Guéguen (2010). vS30, κ, regional attenuation and Mw from small magnitude events accelerograms, Geophys. J. Int. 182, 880–898.10

Hanks, T. C. (1982). f max , Bull. Seismol. Soc. Am. 72, 1867–1879.

Hanks, T.C. & Kanamori, H., 1979. A moment magnitude scale, J. geophys. Res., 84(B5), 2348–2350.

Scherbaum, F., Cotton, F. & Smit, P., 2004. On the use of response spectral-reference data for the selection and ranking of ground-motion models for seismic-hazard analysis in regions of moderate seismicity: the case of rock motion, Bull. seism. Soc. Am., 94(6), 2164–2185.

Scherbaum F., Delavaud E., and Riggelsen C. (2009). Model selection in seismic hazard analysis: An information-theoretic perspective. Bulletin of the Seismological Society of America 99 (6), 3234-3247.

Van Houtte C., Drouet S., and Cotton F. (2011). Analysis of the Origins of κ (Kappa) to Compute Hard Rock to Rock Adjustment Factors for GMPEs. Bulletin of the Seismological Society of America 101, 2926-2941.